POOL BOILING HEAT TRANSFER IN A VERTICAL ANNULUS WITH A NARROWER UPSIDE GAP

MYEONG-GIE KANG
Department of Mechanical Engineering Education, Andong National University
388 Songchun-dong, Andong-city, Kyungbuk, 760-749, Korea
E-mail : mgkang@andong.ac.kr

Received May 15, 2009
Accepted for Publication September 4, 2009

The effects of the narrowed upside gap on nucleate pool boiling heat transfer in a vertical annulus were investigated experimentally. For the study, a stainless steel tube with a diameter of 25.4 mm and saturated water that kept an atmospheric condition were used. The ratio between the gaps measured at the upper and the lower regions of the annulus ranged from 0.18 to 1. Two different lengths of the modified gap also were investigated. The change in heat transfer due to the modified gap became evident as the gap ratio decreased and the length of the gap increased. As the gap ratio became less than 0.51, a significant decrease in heat transfer was observed compared to the plain annulus. The longer gap size resulted in an additional decrease in heat transfer. The major cause for the tendency was attributed to the formation of lumped bubbles around the upper region of the annulus followed by the increased flow friction between the fluid and the surface around the modified gap.

KEYWORDS : Pool Boiling, Vertical Annulus, Upside Flow Area, Gap, Tube, Heat Transfer

1. INTRODUCTION

Since pool boiling has become important for use in fluid flow and heat transfer, the mechanisms of pool boiling have been studied extensively for the past several decades [1]. Recently, pool boiling has been widely investigated in nuclear power plants for potential application to the design of new passive heat removal systems employed in Advanced Light Water Reactors (ALWRs) designs [2]. From reviewing the published results, it can be concluded that one of the most efficient ways to increase the heat transfer rate is to have a confined space. Although many researchers have investigated pool boiling heat transfer by assuming several different geometric parameters, knowledge on pool boiling heat transfer in confined spaces is still quite limited. Studies have shown that the pool boiling phenomena in a confined space are very interesting from the view point of both research and applications. Studies on the crevices can be divided into two categories. One of them is annuli [3-6] and the other is plates [7-9]. In addition to the geometric conditions, the flow to the crevices can be controlled. Some researchers have also restricted the bottom side inflow to the crevices [3,6,7].

It is well known from the literature that the confined boiling is an effective technique that enhances heat transfer. It can result in heat transfer improvements up to 300%-800% at low heat fluxes compared to unconfined boiling [3,7]. The boiling heat transfer coefficient usually increases significantly when the gap size decreases at low heat fluxes whereas the heat transfer coefficient decreases at higher heat fluxes. However, the heat transfer coefficient increases when the gap size decreases to a certain value [3-5,8]. Further decrease in the gap size results in a sudden decrease of the heat transfer coefficient. One of the possible reasons of the deterioration in heat transfer is a formation of big bubbles followed by active bubble coalescence at the upper regions of the annulus [5].

Around the upper region of the annulus, which has a closed bottom, the downward liquid flow interferes with the upward bubble flow. Thereafter, bubbles coalesce to a big lump while fluctuating up and down in the annular gap. Kang [6] published effective results of moving the deterioration point to a higher heat flux and of preventing the occurrence of the critical heat flux. To remove the coalescence of the big bubbles around the upper region of the annulus, Kang [6] controlled the length of the outer tube of the annulus. The major cause of the big bubble formation that results in the deterioration is partly due no inflow occurring through the lower regions of the annulus. Kang [10] identified that the inflow area at the bottom regions of an annulus changed heat transfer coefficients frequently and, moreover, moved the deterioration point of the heat transfer coefficients to the higher heat fluxes.

Summarizing the previous studies about the pool boiling

heat transfer in an annulus, it can be stated that heat transfer coefficients are highly dependent on the geometry and the type of confinement condition. One of the most interesting and important geometric parameters in pool boiling heat transfer is the flow area at the upside region of the annulus. This kind of geometry is generally found in an In-Pile test Section (IPS), which is important in identifying nuclear fuel irradiation behavior at the operating condition of a commercial power plant. Since IPS has several reduced flow areas along the vertical annular length, pool boiling analaysis in the space is of concern. Up to the author's knowledge, no previous results concerning this effect have been published yet. Therefore, the present study aims to investigate the effects of the upside gap geometry on pool boiling heat transfer, which can provide a clue to the thermal design of those kinds of facilities.

2. EXPERIMENTS

A schematic view of the present experimental apparatus and a test section is shown in Fig. 1. The water tank (Fig. 1(a)) was made of stainless steel and had a rectangular cross section (950 × 1300 mm) and a height of 1400 mm. The sizes of the inner tank were 800 × 1000 × 1100 mm (depth × width × height). Four auxiliary heaters (5 kW/heater) were installed at the space between the inside and the outside tank bottoms. The heat exchanging tube was a resistance heater (Fig. 1(b)) made of a very smooth stainless steel tube (heated length $L = 0.5$ m and diameter $D = 25.4$ mm). The surface of the tube was finished through a buffing process to have a smooth surface. Electric power of 220 V AC was supplied through the bottom side of the tube.

The tube outside was instrumented with five T-type sheathed thermocouples (diameter was 1.5 mm). The thermocouple tip (about 10 mm) was brazed on the tube wall. The brazing metal was a kind of brass and the averaged brazing thickness was less than 0.1 mm. The temperature decrease along the brazing metal was calibrated by the one dimensional conduction equation. The water temperatures were measured with six sheathed T-type thermocouples brazed on a stainless steel tube that was placed vertically at a corner of the inside tank. All thermocouples were calibrated at a saturation value (100 °C since all tests were done at atmospheric pressure). To measure and/or control the supplied voltage and current, two power supply systems were used.

For the tests, the heat exchanging tube was assembled vertically at the supporter (Fig. 1(a)) and an auxiliary supporter was used to fix the glass tube (Fig. 1(b)). To make the annular condition, a glass tube of 55.4 mm inner diameter (D_i) and 600 mm length was situated around the heated tube. The gap size ($s = D_i - D)/2$) of the main body of the annulus was 15 mm. To maintain the gap size between the heated tube and the glass tube, a spacer (Fig. 2(b)) was installed at the upper region of the test section. The upside flow space was controlled by flow interrupters (Fig. 2(c)). Three different outside diameters ($d = 40$, 45,

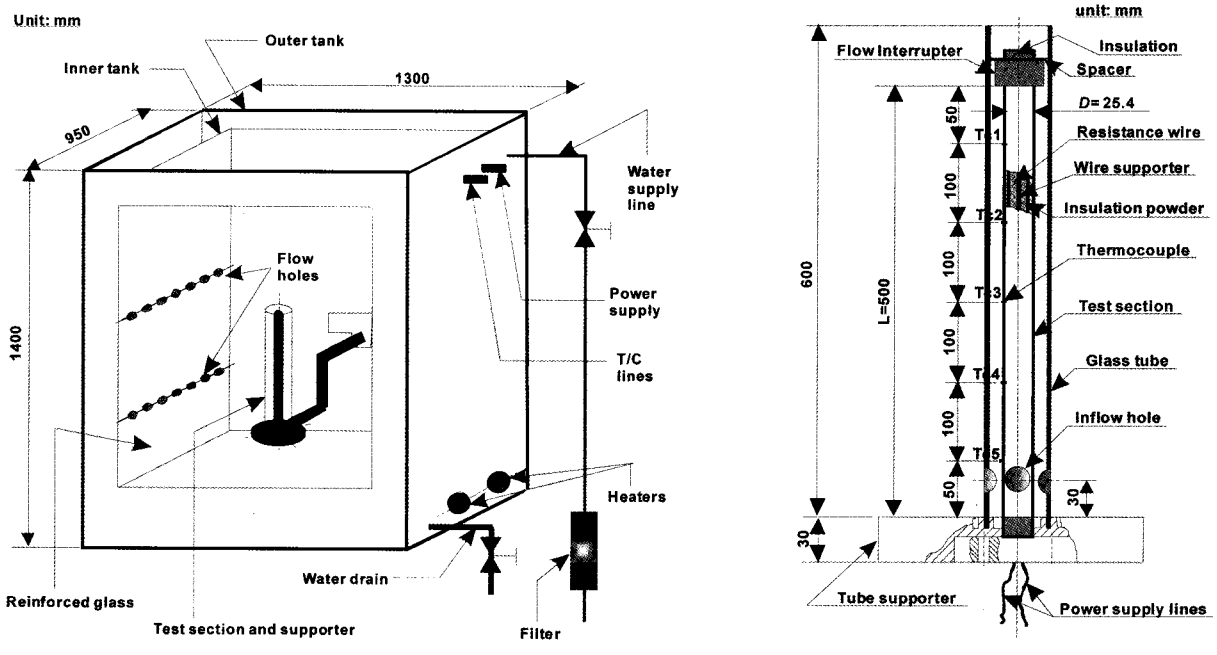

(a) Water Tank

(b) Assembled Test Section

Fig. 1. Schematics of the Experimental Apparatus

and 50 mm) and two different axial lengths (w = 10 and 30 mm) were considered. After installing one of the flow interrupters around the test section, the spacer was screwed down on the test section tightly. Because of the flow interrupter, the gap size around the interrupter ($s_d = D_i - d$) / 2) was different than the gap of the main body. The ratio of the gaps ($s_r = s_d / s$) varied from 0.18 to 1, as shown in Table 1. Among the values, $s_r = 1$ represented the annulus without the flow interrupter. For the tests, the length of the flow interrupter (w) changed, as listed in Table 1.

After the water tank was filled with water until the initial water level reached 1100 mm, the water was then heated by using four pre-heaters at constant power. When the water temperature reached the saturation value, the water was then boiled for 30 minutes in order to remove the dissolved air. The temperatures of the tube surfaces (T_W) were measured when they were at a steady state while the heat flux on the tube surface was controlled with input power.

The heat flux from the electrically heated tube surface was calculated from the measured values of the input power as follows:

$$q'' = \frac{VI}{\pi DL} = h_b \Delta T_{sat} = h_b (T_W - T_{sat}) \quad (1)$$

where V and I are the supplied voltage and current, and D and L are the outside diameter and the length of the heated tube, respectively. T_W and T_{sat} represent the measured temperatures of the tube surface and the saturated water, respectively. Every temperature used in Eq. (1) is the arithmetic average value of the temperatures measured by the thermocouples.

The uncertainties of the experimental data were calculated by using the law of error propagation [11]. The data

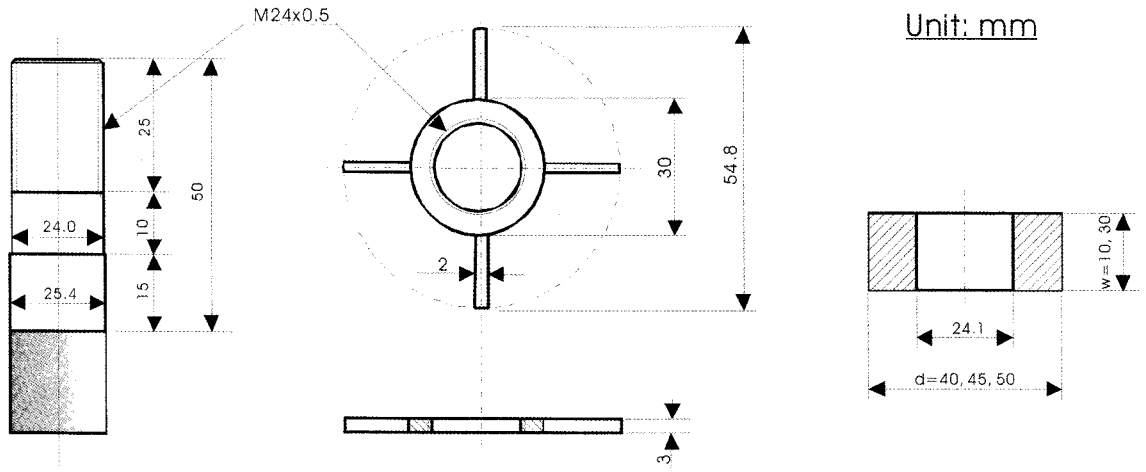

(a) Test Section (b) Spacer (c) Flow Interrupter

Fig. 2. Detailed Views of the Test Tube Upper Regions

Table 1. Test Matrix and q'' Versus ΔT_{sat} Data

d, mm	w, mm	s_d, mm	s_r (=s_d/s)	q'', kW/m^2	Remark	Number of data
-	-	-	-	0-120	Single	12
-	-	15.0	1	0-120	Bottom open	12
40	10	7.7	0.51	0-120	Bottom open	12
45	10	5.2	0.35	0-120	Bottom open	12
50	10	2.7	0.18	0-120	Bottom open	12
40	30	7.7	0.51	0-120	Bottom open	12
45	30	5.2	0.35	0-120	Bottom open	12
50	30	2.7	0.18	0-120	Bottom open	12

acquisition error (A_T, ±0.05 °C) and the precision limit (P_T, ±0.1 °C) were counted for the uncertainty analysis of the temperature. The 95 percent confidence uncertainty of the measured temperature was calculated from $(A_T^2+P_T^2)^{1/2}$ and had the value of ±0.11 °C. The error bound of the voltage and current meters used for the test was ±0.5% of the measured value. Therefore, the uncertainty of the calculated power (voltage × current) was obtained at ±0.7%. Since the heat flux had the same error bound as the power, the uncertainty in the heat flux was estimated to be ±0.7%. When evaluating the uncertainty of the heat flux, the error of the heat transfer area was not counted since the uncertainty of the tube diameter and the length was ±0.1 mm and its effect on the area was negligible. To determine the uncertainty of the heat transfer coefficient, the uncertainty propagation equation was applied on Eq. (1). Since the values of the heat transfer coefficient were the result of the calculation of $q''/\Delta T_{sat}$, a statistical analysis on the results was performed. After calculating and taking the mean of the uncertainties of the propagation errors, the uncertainty of the heat transfer coefficient was determined to be ±6%.

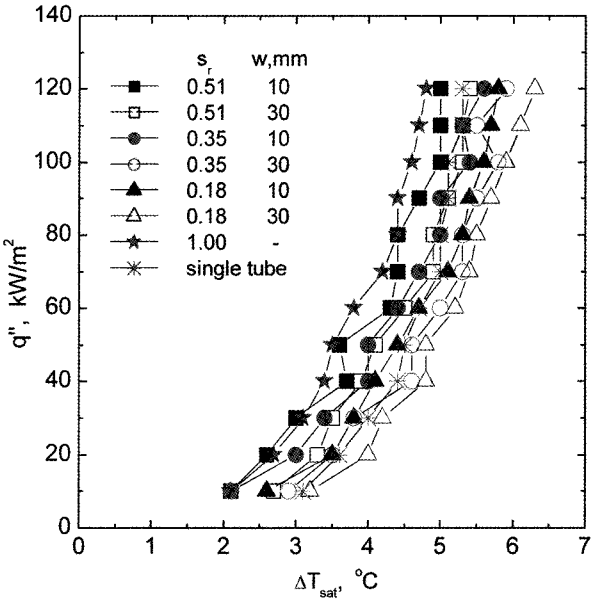

Fig. 3. Curves of q'' Versus ΔT_{sat} Data

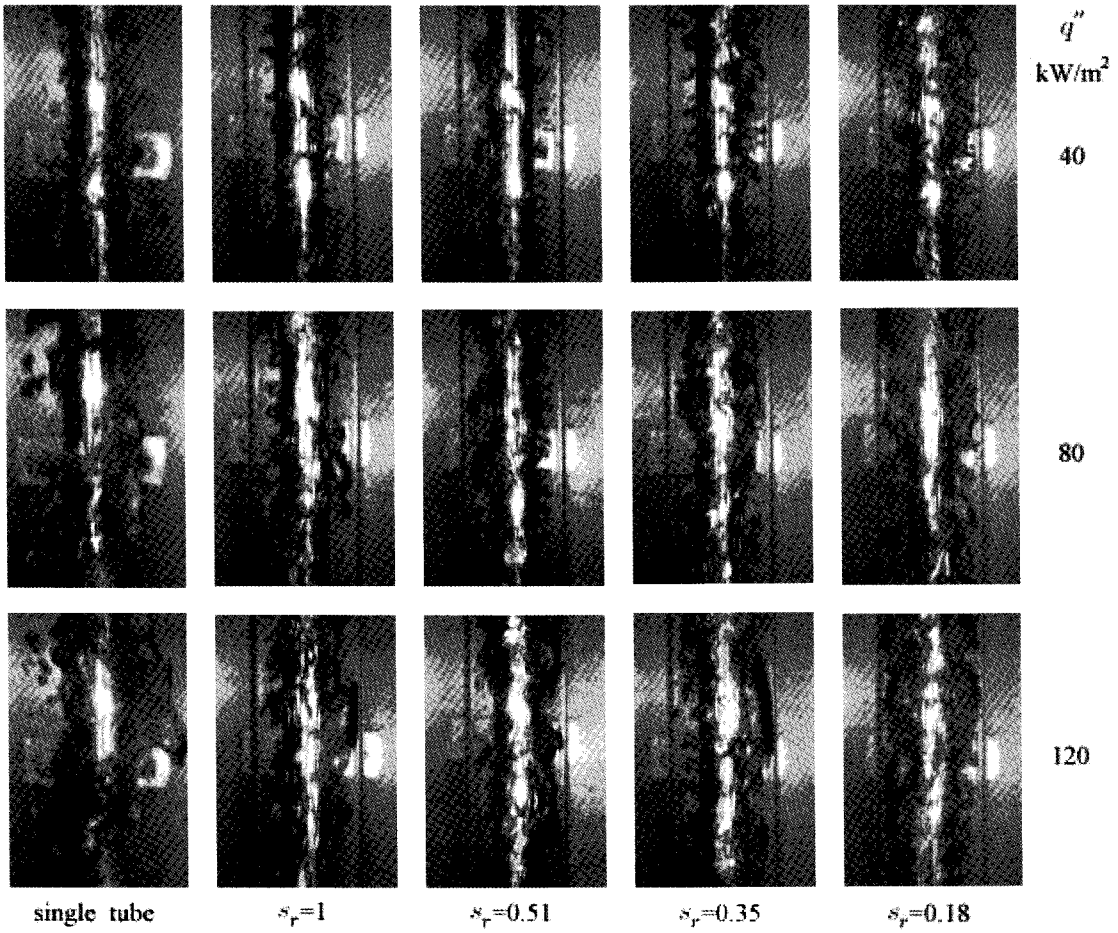

Fig. 4. Photos of Pool Boiling on the Tube Surface as w=10mm

3. RESULTS AND DISCUSSION

Figure 3 shows the variations in heat transfer as the diameter and the length of the flow interrupter changes. Because of the interrupter, the heat transfer rate decreased compared to the rate of the annulus without the interrupter. The smaller gap ratio resulted in a reduced heat transfer. For the given gap ratio and the heat flux, an additional decrease in heat transfer was observed at the longer flow interrupter. For example, when $w=10$ mm, ΔT_{sat} increased only 20.8% (from 4.8 to 5.8 °C) while s_r decreased by 82% (from 1 to 0.18) at the given heat flux ($q''=120$ kW/m^2). As the length changed to 30 mm, the tube wall superheat increased significantly with the same heat flux and the gap ratio. According to Fig. 3, ΔT_{sat} increased more than 31.3 % (from 4.8 to 6.3 °C) when $w=30$ mm. Throughout the entire heat fluxes, the change in ΔT_{sat} became noticeable because of the decrease in s_r and the increase in w. For the shorter ($w=10$ mm) interrupters, the heat transfer rates for the annuli were higher than the single unrestricted tube that had low heat fluxes smaller than 60 kW/m^2. When the gap ratio was $s_r=0.18$ and $w=10$mm, the slopes of q'' versus ΔT_{sat} curve shown in Fig. 3 shifted and crossed the curve of the single unrestricted tube at about $\Delta T_{sat}=4.7$ °C and $q''=60$ kW/m^2. The results for the longer (i.e., $w=$ 30mm) interrupters showed much smaller curve slopes compared to the results for the shorter ones. As the boiling became more vigorous, especially for the smaller gap ratios, heat transfer deteriorated significantly compared to the annulus without the interrupter.

Figure 4 shows some photos of pool boiling for $w=$ 10mm. Those photos were taken around the mid-point of the tube length. The photos of the annuli show big bubbles inside the gap space compared to the single unrestricted tube. For the annulus, the increase in the number and size of the bubbles were clearly observed in the gap space when the value of the gap ratio decreased from 1 to 0.18.

Changes in heat transfer coefficients as the gap ratio increased are plotted in Fig. 5 for the three different heat fluxes. As the gap ratio became less than 0.51, a sudden decrease in heat transfer coefficients was observed, regardless of the heat flux. For the same gap ratio, results for the longer interrupters (i.e., $w=30$mm) showed smaller heat transfer coefficients compared to the results for the shorter ones.

To identify the effects of the interrupter length on heat transfer coefficients, the ratios (i.e., $h_{b,w=30}/h_{b,w=10}$) between the two heat transfer coefficients for the annuli with a different interrupter length are plotted as the heat flux increased. In Fig. 6, the results for the three different gap ratios are shown. Throughout the gap ratios, the calculated results of $h_{b,w=30}/h_{b,w=10}$ were less than 1, regardless of the heat fluxes. The tendency was clearly observed as the heat flux was less than 60 kW/m^2. For the heat fluxes larger than 80 kW/m^2, the ratios of $h_{b,w=30}/h_{b,w=10}$ showed a tendency of converging at a value around 0.95 according to the gap ratio.

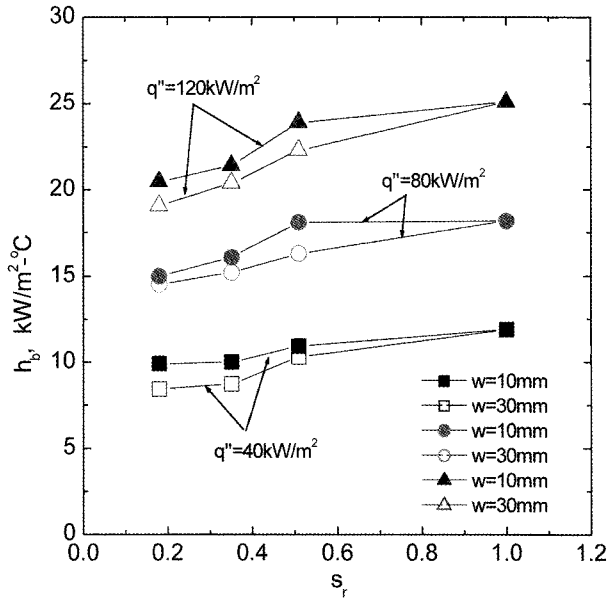

Fig. 5. Curves of h_b Versus S_r

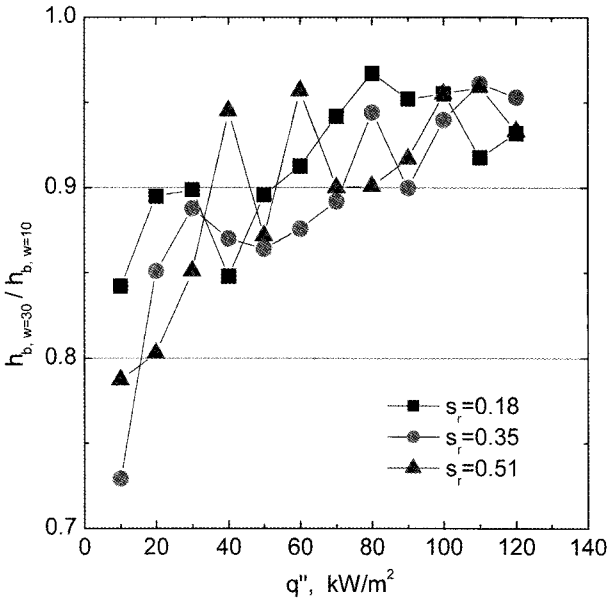

Fig. 6. Variations in Heat Transfer Coefficients Versus Heat Fluxes

The reason for the above mentioned results may be attributable to the following phenomena:

(1) The flow interrupter obstructed the outward bubble flow from the annulus. Because of the interrupter, a kind of bottleneck was created just below the interrupter. Then, the detached bubbles that came from the lower part of the tube became stagnant for a while and accumulated at the upper region of the annulus. During the stay, the bubbles coalesced together and grew to a

big lump of bubbles. Thereafter, the upward rising velocity of the fluid decreased because of the lump. Since the major heat transfer resistance was the heat conduction across the liquid film, the reduced film thickness under the bubbles increased the heat transfer coefficient [3]. When the fluid velocity decreased, the shear stress on the liquid film at the heated surface decreased and, accordingly, the thickness of the liquid film increased. The thickened film decreased heat transfer. The tendency of decreasing the heat transfer due to the decrease in the fluid velocity was also observed in the forced convective nucleate boiling [12]. The size of the bubble lump increased until the amount of the buoyancy was enough to escape from the gap space. The increase in the heat flux led to a decrease in the heat transfer rate since more bubbles were generated on the tube surface.

(2) As the gap ratio decreased, even bigger bubbles were generated underneath the interrupter. These bigger bubble lumps restricted the upstream flow from the lower regions of the annulus to the free water surface. Thereafter, the decrease in heat transfer rate resulted from the decrease in the fluid velocity. The same thing was true for the longer interrupter. As the length of the flow interrupter increased, the length of the annulus with a narrower gap increased as well. This created stronger flow friction between the outward fluid and the wall than the shorter interrupter. As a result of the flow restriction, heat transfer coefficients decreased more, followed by a decrease in the fluid velocity, which was the result from the generation of big bunches of bubbles.

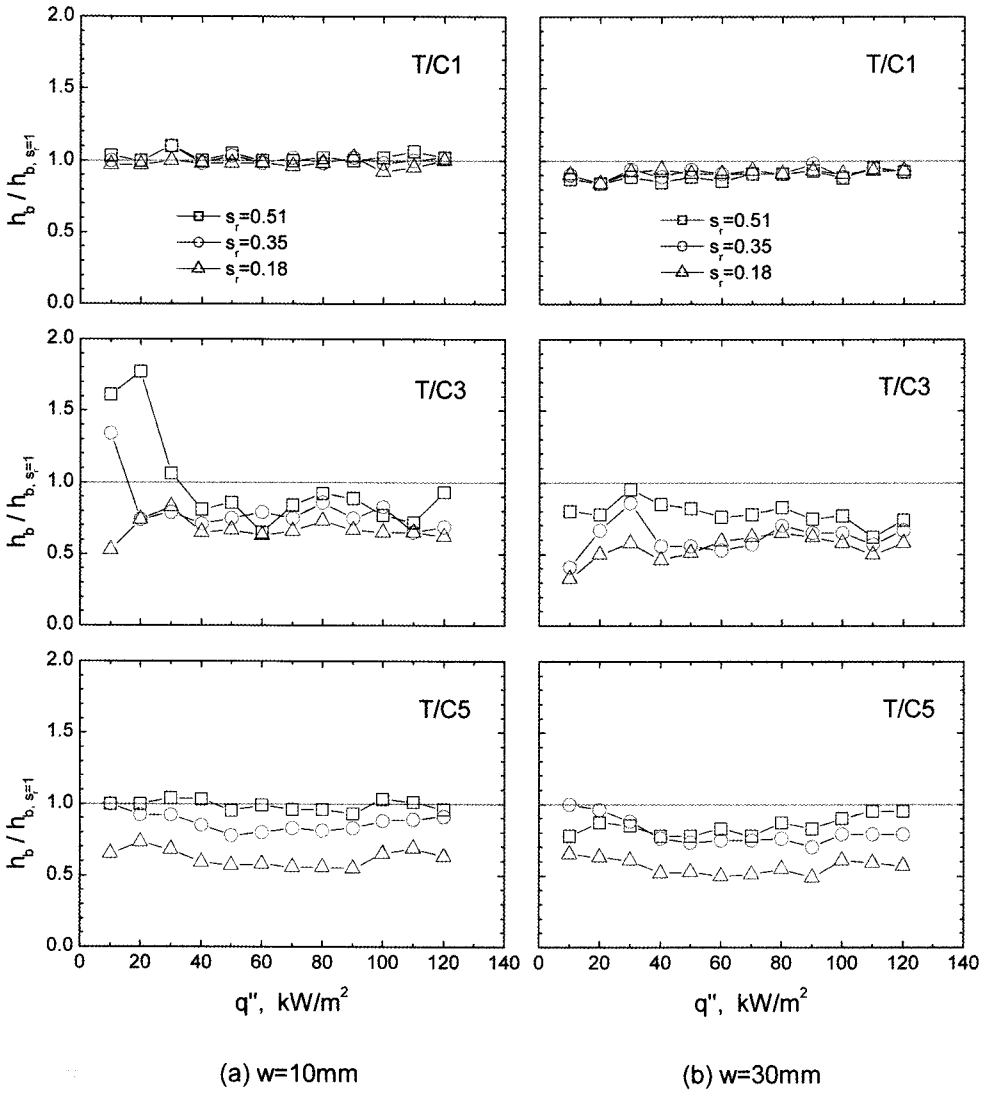

Fig. 7. Plots of $h_b/h_{b,s_r=1}$ Versus q'' at Local Points on Tube Surface in an Annulus

The mechanisms that affected heat transfer were obtained by the local heat transfer coefficients. Local heat transfer coefficients at the locations of the thermocouple #1, #3, and #5 (see Fig. 1(b) to identify thermocouple locations on the tube surface) are shown in Fig. 7 as the heat flux is increasing. To compare those results between the annuli with or without the flow interrupter, the ratios between the heat transfer coefficient with the flow interrupter and the heat transfer coefficient without the flow interrupter (i.e., $h_{b,s_r=1}$) were plotted. Results for the three different gap ratios were compared at the thermocouple locations. The ratios were almost 1 at the uppermost location (T/C1). However, the ratios got smaller than 1 at the lower regions of the tube (i.e., T/C3 and T/C5). Since fluid convection was an important mechanism for heat transfer, the decrease in heat transfer coefficients due to the reduced flow velocity was clearly observed at the lower regions. For the longer flow interrupter, the tendency was more evident. At the uppermost location (T/C1) of the tube, bigger size bubbles gathered around the region and the location was relatively free from the convection term. Therefore, relatively small changes in heat transfer coefficients were observed, in spite of the adoption of the flow interrupter.

To obtain parametric effects of the gap ratio and the interrupter length on heat transfer coefficients, an empirical correlation was suggested. As listed in Table 1, a total of 84 data points were obtained for the heat flux versus the wall superheat for various combinations of the annular gap and the flow interrupter. Data points for the single tube were not included for the development of the correlation. To take into account the effects of the gap size and the heat flux, a simple correlation was thought as $h_b = C_1 q''^{C_2} s_r^{C_3} w_r^{C_4} L_r^{C_5}$. Using the present experimental data and the statistical analysis computer program (which used the least square method as a regression technique), an empirical correlation was obtained as follows:

$$h_b = 0.65 q''^{0.68} s_r^{0.11} w_r^{0.07} L_r^{0.12}$$

$$L_r = L/w, \quad s_r = s_d/s, \quad w_r = w/d \qquad (2)$$

In the above equation, the dimensions for h_b and q'' were kW/m^2-°C and kW/m^2, respectively. L_r, S_r, and w_r were dimensionless. The heat transfer coefficient increased in proportion to $L_r^{0.12}$, $s_r^{0.11}$ and $w_r^{0.07}$. The results of the curve fitting are listed in Table 2. Apparently, the correlation only applied for the testing pressure and parameters shown in Table 1. The above correlations were only applicable for water on a stainless steel surface.

To confirm the validity of the empirical correlation, a statistical analysis on the ratios of the measured to calculated heat transfer coefficients (i.e. $h_{b,\exp erimental} / h_{b,correlation}$) was performed. The calculated standard deviation was 0.049.

Table 2. Results of Curve Fitting [$h_b = C_1 q''^{C_2} s_r^{C_3} w_r^{C_4} L_r^{C_5}$]

Parameter	Parametric value	Standard deviation
C_1	0.65249e+00	0.85592e-01
C_2	0.67962e+00	0.86577e-02
C_3	0.11322e+00	0.18302e-01
C_4	0.74936e-01	0.42189e-01
C_5	0.12363e+00	0.42944e-01

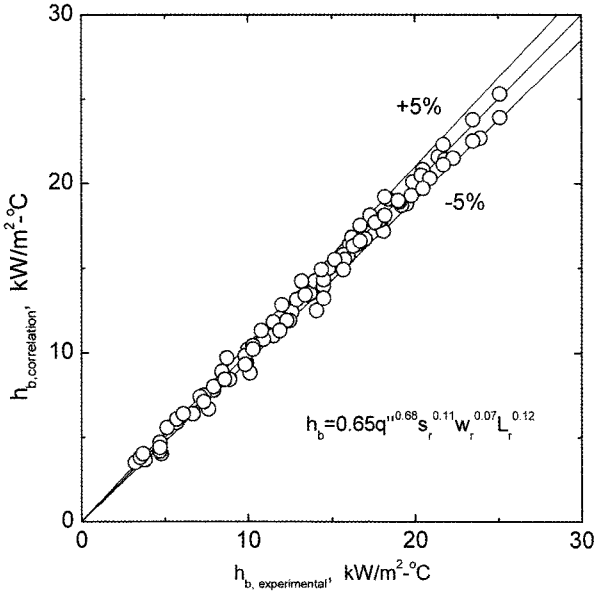

Fig. 8. Comparison of the Experimental Data to the Calculated Heat Transfer Coefficients

A comparison between the heat transfer coefficients from the tests ($h_{b,\exp erimental}$) and the correlation ($h_{b,correlation}$) is shown in Fig. 8. This figure indicates that the scattering bounds of the present experimental data were ±5%, with some exceptions, from the fitted curve of Eq. (2). Therefore, it can be said that the developed correlation predicted the data with a reasonable error bound. Although the number of the data points used for the development was not enough for the general application, the results would be useful in gaining a preliminary understanding of the narrowed gap before adopting a flow interrupter into the thermal design.

4. CONCLUSIONS

To investigate the effects of the upside gap geometry on pool boiling heat transfer in a vertical annulus, the size and the length of the gap at the upper region of the annulus

were regulated by using the flow interrupters. For the test, a heated tube with a diameter of 25.4 mm and the water at atmospheric pressure were used. The major conclusions of the study are as follows:

1) The adoption of the flow interrupter in an annulus decreased heat transfer coefficients compared to the annulus without the flow interrupter. As $s_r < 0.51$ and w =30 mm, a noticeable decrease in heat transfer coefficients was observed.
2) One of the possible causes of the heat transfer deterioration was recognized to be the reduction of flow velocity due to the sizable bubble formation beneath the interrupter.
3) To quantify the effects of the upside narrower gaps on heat transfer, an empirical correlation was suggested, which predicts the experimental data in a reasonable error bound. According to the correlation, the heat transfer coefficients was proportional to $L_r^{0.12}$, $s_r^{0.11}$ and $w_r^{0.07}$.

REFERENCES

[1] M. H, Chun and M. G. Kang, "Effects of Heat Exchanger Tube Parameters on Nucleate Pool Boiling Heat Transfer," *ASME J. Heat Transfer*, **120**, 468 (1998).

[2] M. Shoji, "Studies of Boiling Chaos: a Review," *Int. J. Heat Mass Transfer*, **47**, 1105 (2004).

[3] S. C. Yao and Y. Chang, "Pool Boiling Heat Transfer in a Confined Space," *Int. J. Heat Mass Transfer*, **26**, 841 (1983).

[4] Y. H. Hung and S. C. Yao, "Pool Boiling Heat Transfer in Narrow Horizontal Annular Crevices," *ASME J. Heat Transfer*, **107**, 656 (1985).

[5] M. G. Kang and Y. H. Han, "Effects of Annular Crevices on Pool Boiling Heat Transfer," *Nuclear Engineering and Design*, **213**, 259 (2002).

[6] M. G. Kang, "Pool Boiling Heat Transfer on a Vertical Tube with a Partial Annulus of Closed Bottoms," *Int. J. Heat Mass Transfer*, **50**, 423 (2007).

[7] J. Bonjour and M. Lallemand, "Flow Patterns During Boiling in a Narrow Space between Two Vertical Surfaces," *Int. J. Multiphase Flow*, **24**, 947 (1998).

[8] Y. Fujita, H. Ohta, S. Uchida, and K. Nishikawa, "Nucleate Boiling Heat Transfer and Critical Heat Flux in Narrow Space between Rectangular Spaces," *Int. J. Heat Mass Transfer*, **31**, 229 (1988).

[9] J. C. Passos, F. R. Hirata, L. F. B. Possamai, M. Balsamo, and M. Misale, "Confined Boiling of FC72 and FC87 on a Downward Facing Heating Copper Disk," *Int. J. Heat Fluid Flow*, **25**, 313 (2004).

[10] M.G. Kang, "Pool Boiling Heat Transfer in a Vertical Annulus as the Bottom Inflow Area Changes," *Int. J. Heat Mass Transfer*, **51**, 3369 (2008).

[11] H.W. Coleman and W.G. Steele, *Experimentation and Uncertainty Analysis for Engineers*, 2nd Ed., John Wiley & Sons (1999).

[12] W.M. Rohsenow, "A Method of Correlating Heat-transfer Data for Surface Boiling of Liquids," *ASME J. Heat Transfer*, **74**, 969 (1952).